The Role of Cystine Knots in Collagen Folding and Stability, Part II.[+] Conformational Properties of (Pro-Hyp-Gly)$_n$ Model Trimers with N- and C-Terminal Collagen Type III Cystine Knots**

Dirk Barth,[a] Otto Kyrieleis,[a] Sabine Frank,[b] Christian Renner,[a] and Luis Moroder*[a]

Abstract: In mature collagen type III the homotrimer is C-terminally cross-linked by an interchain cystine knot consisting of three disulfide bridges of unknown connectivity. This cystine knot with two adjacent cysteine residues on each of the three α chains has recently been used for the synthesis and expression of model homotrimers. To investigate the origin of correct interchain cysteine pairings, (Pro-Hyp-Gly)$_n$ peptides of increasing triplet number and containing the biscysteinyl sequence C- and N-terminally were synthesised. The possibilities were that this origin may be thermodynamically coupled to the formation of the collagen triple helix as happens in the oxidative folding of proteins, or it could represent a post-folding event. Only with five triplets, which is known to represent the minimum number for self-association of collagenous peptides into a triple helix, air-oxidation produces the homotrimer in good yields (70%), the rest being intrachain oxidised monomers. Increasing the number of triplets has no effect on yield suggesting the formation of kinetically trapped intermediates, which are not reshuffled by the glutathione redox buffer. N-terminal incorporation of the cystine knot is significantly less efficient in the homotrimerisation step and also in terms of triple-helix stabilisation. Compared to an artificial C-terminal cystine knot consisting of two interchain disulfide bridges, the collagen type III cystine knot produces collagenous homotrimers of remarkably high thermostability, although the concentration-independent refolding rates are not affected by the type of disulfide bridging. Since the natural cystine knot allows ready access to homotrimeric collagenous peptides of significantly enhanced triple-helix thermostability it may well represent a promising approach for the preparation of collagen-like innovative biomaterials. Conversely, the more laborious regioselectively formed artificial cystine knot still represents the only synthetic strategy for heterotrimeric collagenous peptides.

Keywords: collagen · cystine knot · peptides · protein folding · triple helix

Introduction

The homotrimeric collagen type III contains at the C-terminus two adjacent cysteine residues which, upon initial trimerisation of the α chains by the non-collagenous prodomains, form an interchain disulfide knot of unknown connectivity.[1] This cystine knot, which is C-terminally extended by a non-collagenous sequence portion, as well as an identical C-terminal cystine knot present in the amino-terminal segment of type III procollagen (Col 1-3) were found to provide an efficient nucleus for triple-helix propagation from the C- to the N-terminus in a zipper-like mechanism.[2] Modelling of this cystine knot, which is generated by interchain-disulfide bridging of two adjacent cysteine residues located on each of the three identical α-chains, suggested that only one of the eight possible isomers can be accommodated into a triple helix.[2b] The chemistry so far available for regioselective interchain-cysteine pairings is, however, insufficient to cross-link three peptide chains by three disulfide bonds. Therefore, in our previous studies on synthetic collagen peptides we used a simplified cystine knot consisting of only two disulfides for the selective assembly of three different peptide chains into heterotrimeric collagen molecules in the desired chain register.[3]

Recently, a (Gly-Glu-Arg)$_{15}$ peptide C-terminally extended by the sequence Gly-Pro-Cys-Cys-Gly of collagen type III was synthesised and oxidised under GSH/GSSG catalysis as well

[a] Prof. Dr. L. Moroder, Dipl. Chem. D. Barth, Dipl. Chem. O. Kyrieleis, Dr. C. Renner
Max-Planck-Institute für Biochemie
Am Klopferspitz 18 A, 82152 Martinsried (Germany)
Fax: (49) 89-8578-2847
E-mail: moroder@biochem.mpg.de

[b] Dr. S. Frank
Department für Biophysikalische Chemie
Biozentrum, Universität Basel, 4056 Basel (Switzerland)
E-mail: sabine.frank@unibas.ch

[+] For Part I see ref. [6].

[**] **Abbreviations:** Standard abbreviations are used as recommended by the IUPAC-IUB commission on biochemical nomenclature and the ACS Style Guide. All amino acids are of L configuration. Additional abbreviations: CVFF, consistent valence force field; DBU, 1,8-diazabicyclo[4.4.0]undec-7-ene; DIEA, diisopropylethylamine; DMAP, 4-dimethylaminopyridine; DMF, dimethylformamide; GSH glutathione; HBTU, *N*-[(1*H*-benzotriazol-1-yl)(dimethylamino)-methylene]-*N*-methylmethanaminium hexafluorophosphate *N*-oxide; HOBt 1-hydroxybenzotriazole; NMP, *N*-methylpyrrolidinone; TFE, 2,2,2-trifluoroethanol; TFFH, fluoro-*N*,*N*,*N*′,*N*′-tetramethylformamidinium hexafluorophosphate; TOCSY, total correlation spectroscopy.

 DOI: 10.1002/chem.200304918

as in the presence of protein-disulfide isomerase to produce a homotrimeric model collagen peptide for studying pH effects on the stability of a triple-helix devoid of prolines.[4] Similarly, a polypeptide chain consisting of $(Gly\text{-}Pro\text{-}Pro)_n$ and elongated C-terminally with the Gly-Pro-Cys-Cys-$(Gly)_3$ sequence was expressed in *E. coli* and successfully oxidised under GSH/GSSG catalysis into the desired homotrimer.[5] The oxidation product was characterised as a trimer by SDS-Page and analytical ultracentrifugation, and it exhibited concentration-independent thermal unfolding and refolding kinetics typical of cross-linked collagen peptides. The question of whether oxidation of the monomeric species leads to a unique C-terminal cystine knot as suggested from the modelling experiments[2b] was not addressed in these studies.

This successful oxidative assembly of homotrimeric collagenous peptides compelled us to use synthetic $(Pro\text{-}Hyp\text{-}Gly)_n$ peptides of increasing chain length to compare the triple-helix inducing/stabilising effects of this natural cystine knot with the effects of the simplified artificial one used in the preceding article.[6] Moreover, oxidative refolding experiments with such peptides of increasing (Pro-Hyp-Gly) triplet numbers were expected to address the question as to what extent optimally matched self-associated trimers in equilibrium with nonstructured monomers and mismatched triple helices is affecting the yields of correctly oxidised trimers.

In the case of collagen type XIII even N-terminal nucleation of the triple-helical structure has been proposed[7] and numerous conformational studies on collagen model peptides have employed synthetic collagenous trimers N-terminally cross-linked on templates.[8] Most recently, even the native collagen type III cystine knot has been incorporated N-terminally into expressed constructs with $(Gly\text{-}Pro\text{-}Pro)_{10}$, and folding rates were found to be comparable to those of the C-terminally cross-linked collagen peptides.[9] Nonetheless, the additional aim of this study was to further analyse the effect of an N-terminal collagen type III cystine knot on the conformational stability of related collagenous trimers.

For this purpose the trimers **I**–**V** in Figure 1 were designed for oxidative experiments and for comparative analysis with trimer **VI** which was synthesised and characterised in its triple-helical structure in the preceding article.[6] We demonstrate that the monomeric species have to prefold into the triple helix to allow an oxidative assembly to the cross-linked trimers in good yields. It is also apparent that the C-terminal knot is significantly more efficient than the N-terminal, at least according to our design of the monomeric species containing the two adjacent cysteine residues at the C- or N-terminus, respectively.

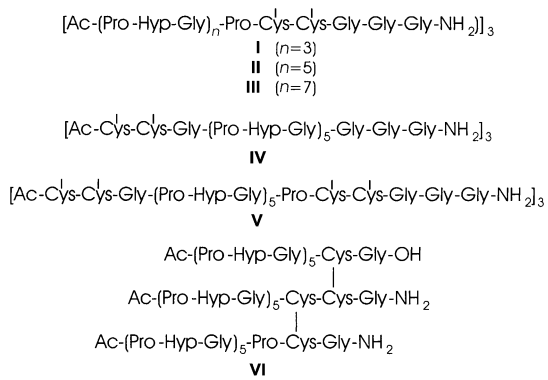

Figure 1. Sequence composition of the homotrimers **I**–**V** whose syntheses were attempted or carried out in the present study; heterotrimer **VI** with the C-terminal artificial cystine knot[6] is reported for comparison.

Results

Synthesis of the trimers

Design of the cystine knots: For the design of trimers **I**–**III** with the C-terminal cystine knot (Figure 1) the residues Yaa and Gly of one classical collagen repeat (Xaa-Yaa-Gly) were replaced by cysteines. The sequence was extended C-terminally with glycines to interrupt the collagenous sequence composition in analogy to the C-terminus of collagen type-III[1] and to the previously reported collagenous peptides containing this cystine-cross-linking system.[4, 5] To induce triple-helix nucleation at the N-terminus, in trimer **IV** (Figure 1) the cysteine residues were placed in the Xaa-Yaa positions of the triplet, since it is well known that replacement of the crucial Gly residue with other amino acids leads to distortion of the collagen structure because of steric clashes.[10] This design, however, differs from that applied by Frank et al. who introduced the dipeptide spacer Gly-Ser between the two adjacent cysteines and the first (Gly-Pro-Pro) repeat.[9] Finally, for cross-linking the α chains both at the N- and C-termini, a combination of both cystine knots was implemented in trimer **V**.

Oxidation experiments: The single chains were synthesised on solid supports by optimised procedures[6] using *S-tert*-butylthio protection for the cysteine residues. The tripeptide derivative Fmoc-Pro-Hyp(*t*Bu)-Gly-OH was used as the synthon for $(Pro\text{-}Hyp\text{-}Gly)_n$ chain elongations according to Fmoc/*t*Bu chemistry. Oxidation of the fully deprotected single chains to form the trimers was carried out under slightly basic conditions in the presence and absence of glutathione (Scheme 1).

The intrinsic ability of the single chains to self-associate into triple-helical homotrimers was found to be crucial in this oxidation/trimerisation step. In fact, the CD spectrum of peptide **1a** with its $(Pro\text{-}Hyp\text{-}Gly)_3$ sequence, at 1 mM concentration in water, is not consistent with the presence of triple-helical homotrimers, in full agreement with previous reports on similar collagenous $(Gly\text{-}Pro\text{-}Hyp)_n$ peptides of increasing triplet numbers.[8b, 11] Thus, even upon equilibration of the peptide **1b** at 4 °C for several hours, its exposure to oxidising conditions at 7–8 °C led to a product mixture in which the desired trimer **I** could not be detected by LC-MS. Conversely, pre-equilibration of peptide **2a**, which contains five (Pro-Hyp-Gly) repeats, at low temperature and at 1 mM concentration yields a CD spectrum that reflects a high content of triple helix with a melting temperature of 20.3 °C (Table 1). This value is very similar to that reported for the related peptide Ac-$(Gly\text{-}Pro\text{-}Hyp)_5$-$NH_2$ at 0.2 mg mL^{-1} concentration in water.[8b] Thus, performing the oxidation experi-

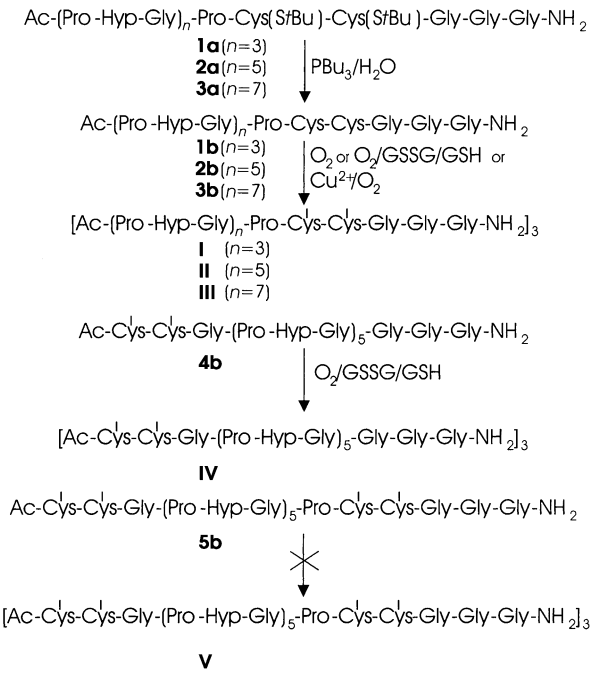

Scheme 1. Oxidative assembly of [Pro-Hyp-Gly]$_n$-containing monomers into the homotrimers **I**–**V**.

Table 1. Thermodynamic parameters extracted from the thermal denaturation curves monitored by CD at 225 nm for the collagen peptides in A) 20 mM phosphate containing 150 mM NaCl, pH 7.2; B) 20 mM phosphate buffer, pH 3.0, containing 1 mM $CuCl_2$, and C) 20 mM phosphate buffer, pH 3.0.

Collagen peptides	Solvent	T_m [°C]	ΔH_{VH} [kJ mol^{-1}]	ΔS_{VH} [J mol^{-1}K^{-1}]
single chain **2a**[a]	A	20.3	+191	+651
trimer **II**[b]	A	68.1	+179	+525
	B	68.0	+179	+525
	C	69.0	+173	+507
trimer **IV**[b]	B	58.4	+131	+397
trimer **VI**[b,c]	C	56.3	+206	+624

[a] Concentration 1×10^{-3} M. [b] Concentration 4×10^{-5} M. [c] Reported from the preceding article[6] for comparison.

ments at 1 mM concentration of **2b** in 25 mM ammonium acetate (pH 8) and at a temperature far below the T_m value, that is at 7–8 °C, most of the substrate was expected to be in the triple-helical structure. In fact, simple air oxidation of **2b** generates a product distribution consisting on average of about 70% trimer **II**, the remaining product being essentially oxidised monomer. The product distribution was not affected by the pH value in the range 7 to 9, although at higher pH values, as expected, oxidation rates were enhanced. Oxidation in the presence of GSH/GSSG (peptide/GSH/GSSG ratio of 1:9:0.9) to possibly reshuffle unproductive oxidation intermediates was found to occur at significantly slower rates, but again without appreciable effect on the product distribution. Performing the experiment in the presence of Cu^{2+} or other metal ions to catalyse the thiol oxidation,[12] the oxidation rates were neither enhanced, nor were the yields of trimer **II** affected.

An increase in the yield of trimer formation was expected for peptide **3b** with its seven (Pro-Hyp-Gly) repeats. The triple-helix stability of the self-associated trimer (1 mM concentration of **3a** in 20 mM phosphate buffer containing 150 mM NaCl, pH 7.2) is significantly increased ($T_m = 41.6$ °C), but the resulting product distribution was found to be very similar to that determined for peptide **2b** with about 70% trimer **III**. A possible explanation could be the high aggregation tendency observed for both the self-associated homotrimeric peptide **3b** and trimer **III** (see below).

Oxidation of peptide **4b** which exhibits an identical intrinsic ability to self-associate into a structured homotrimer as peptide **2b**, generates the desired trimer **IV** with the N-terminal cystine knot in only very low yields. In fact, performing this oxidation under the identical conditions used for peptide **2b** in the absence as well as in the presence of glutathione redox buffer, a product distribution of oxidised monomer/dimer/trimer of approximately 80:10:10 and traces of tetramer was obtained as estimated from the peak areas of the chromatographic elution profile. The identity of the products was verified by LC-MS. Finally, even worse results were obtained in the attempts to produce trimer **V** with both an N- and C-terminal cystine knot by oxidation of peptide **5b**. A complex product mixture was generated which could not be resolved chromatographically into the single components and which probably consists mainly of oligomers.

Analytical characterisation of the trimers: Since the cystine connectivities of the C-terminal cystine knot of collagen type III are so far unknown, modelling experiments were performed which suggest that among the eight possible isomers for the three cross-linked peptide chains by three disulfides, two are the most plausible in terms of steric compatibility when placed at the C-terminus of a triple helix. The two isomers are shown in Scheme 2.

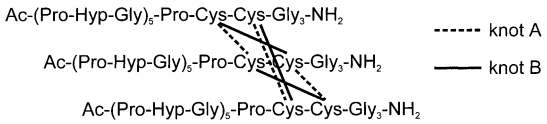

Scheme 2. The two most plausible cystine connectivities knots A and B for trimer **II** as deduced from molecular modelling. Knot A corresponds to the previously-proposed disulfide cross-links.[2b]

The observation that the self-associated homotrimers and the oxidised trimers differ only slightly in their chromatographic properties upon HPLC analysis was not fully unexpected. Therefore, it may also be assumed that different cystine knots would not affect the chromatographic behaviour sufficiently to allow a clear resolution of potential isomers. As a consequence, particular attention was paid to analysing the presence and homogeneity of the cystine knot in the isolated trimers. The chromatographically-isolated products **II**, **III** and **IV** were found to elute as single peaks in size-exclusion chromatography and to behave as homogeneous materials when studied by HPLC. ESI-MS and, particularly, the isotope pattern of FT-ICR-MS confirmed the disulfide-cross-linked trimeric composition of the compounds as illustrated, for example, for trimer **II**, in Figure 2. Although even the NMR spectra were consistent with a single set of cystine connectiv-

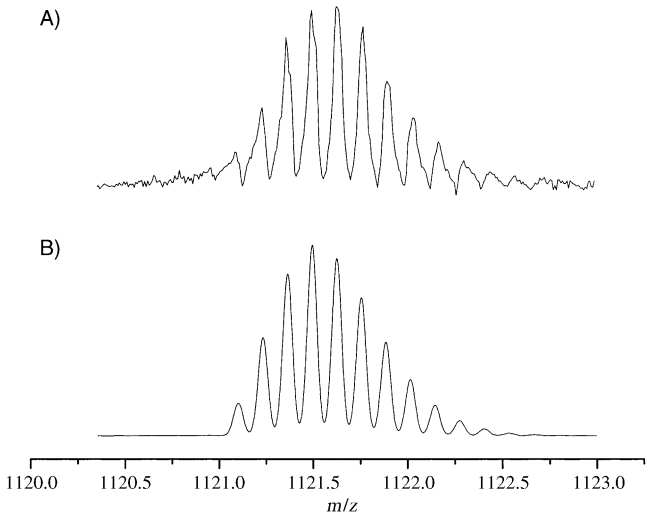

Figure 2. A) Expansion of the region including the $[M+5H]^{5+}$ peak of homotrimer **II** in the FT-ICR-MS spectrum; B) theoretical isotope distribution of the 5-fold charged homotrimer.

ities (see below), the unambiguous proof for the presence of a single cystine knot isomer can only be expected from X-ray crystallographic analysis.

Crystallisation of trimers II and III

From the crystallisation experiments performed so far, non-refracting rod-like crystals were obtained with trimer **II** (Figure 3a) whereas trimer **III** formed essentially fibrils (Figure 3b).

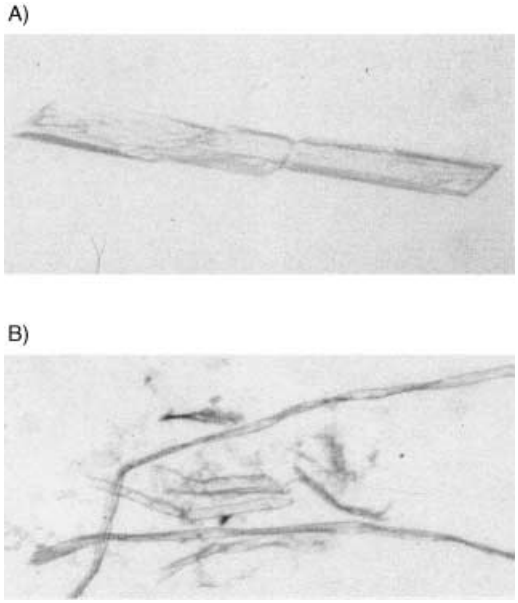

Figure 3. A) Crystals of trimer **II** and B) fibrils of trimer **III**.

This preferred formation of fibrils fully agrees with the observed high tendency of peptide **3b** and trimer **III** to aggregate in solution (see above). The increased refracting power of crystals of $(Pro\text{-}Pro\text{-}Gly)_{10}$ grown under microgravity conditions allowed to determine the correct unit-cell parameters and to derive a model for packing of the collagen molecules which involves direct head-to-tail interactions of the charged N- and C-termini of the triple helices.[13] Most probably an identical organisation of the molecules occurs in crystals grown under normal conditions for $(Pro\text{-}Pro\text{-}Gly)_{10}$ and $(Pro\text{-}Hyp\text{-}Gly)_{10}$.[14] Possibly such organisation favours crystallisation and simultaneously prevents formation of fibrils which were, however, observed in the case of the non-charged trimer **III**. The different behaviour of trimers **II** and **III**, both folded into highly stable triple helices (see below), would suggest the need for a critical length of the rod-shaped molecules for their association into fibrils. This is favoured by water-mediated hydrogen bonding between polar groups[15] such as the Hyp residues present in trimer **III** in a regular pattern.

Conformational properties of the collagenous peptides

A very strong increase in thermal stability of the triple-helical structure is induced by the collagen type III C-terminal knot. This is to be expected on the basis of our previous studies of collagenous peptides cross-linked with a C-terminal artificial cystine knot[3, 6] as well as from studies on trimeric collagenous peptides cross-linked on various templates.[8, 16] This effect is well illustrated in Figure 4 where thermal unfolding of the

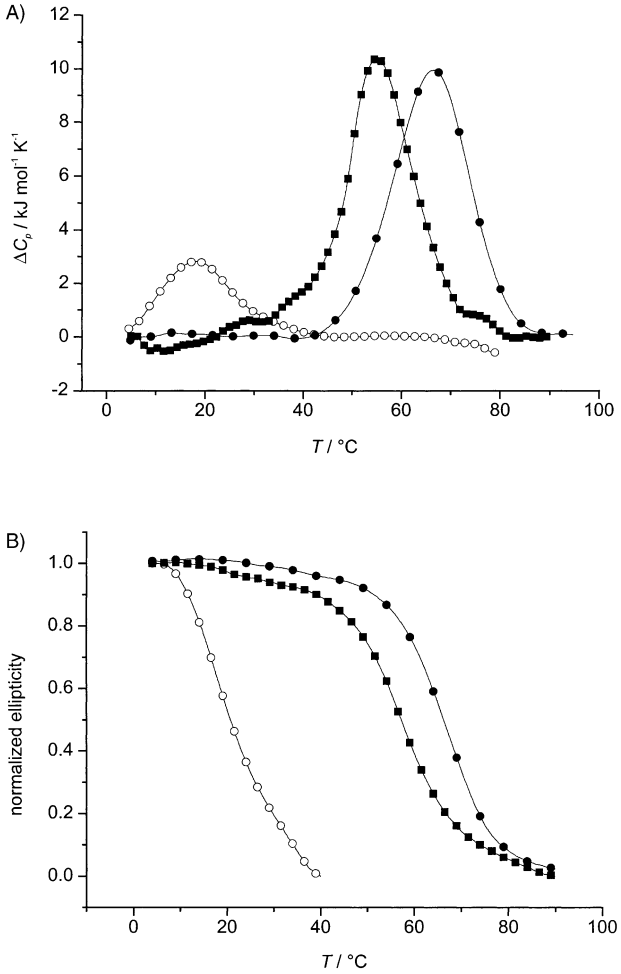

Figure 4. Thermal unfolding of the self-associated monomer **2a** at 1×10^{-3} M (○), trimer **II** (●) and trimer **VI** (■) at 4×10^{-5} M concentration in 20 mM phosphate buffer (pH 3) as monitored by A) DSC and B) CD at 225 nm; the transition curves of trimer **VI** from the preceding article[6] are reported for comparison.

self-associated peptide **2a** is compared to trimer **II**. To allow for a fast equilibration of the peptide **2a**,[17] high peptide concentrations are required. Thus a 1 mM solution of **2a** was used, whereas for the cross-linked trimer **II** where rate constants of the folding and unfolding processes are concentration independent, the concentration was lowered to 4×10^{-5} M. A substantially enhanced T_m value of 68 °C was determined in buffered solution (pH 7.2) for trimer **II** as compared to 20.3 °C for the non-cross-linked peptide **2a** (Table 1). Almost identical transition curves were registered in water (data not shown). It is noteworthy that the triple-helix structure of the (Pro-Hyp-Gly)$_5$ portion of trimer **II** with its native cystine knot is also significantly more stable than that of trimer **VI** cross-linked by the artificial cystine knot (Figure 4 and Table 1).

As expected from the melting temperature of the self-aggregated peptide **3a** with its seven (Pro-Hyp-Gly) triplets ($T_m = 41.6$ °C), for trimer **III** the triple-helix stability reaches a T_m value of 81.5 °C which is very similar to that reported for the recombinant (Pro-Pro-Gly)$_{10}$ with the C-terminal cystine knot ($T_m = 82$ °C).[5] Surprisingly, even at 4×10^{-5} mM concentration in water and in phosphate buffer at both pH 7.2 and 3.0, trimer **III** exhibits a high tendency to aggregate as evidenced by the strong scattering in the far UV. As a consequence, thermodynamic parameters were not derived from CD thermal transition curves at pH 7.2 and 3.0.

A comparison of the conformational stability induced by the N- and C-terminal cystine knot, respectively, (Figure 5) clearly revealed that the latter cross-linking in trimer **IV** is

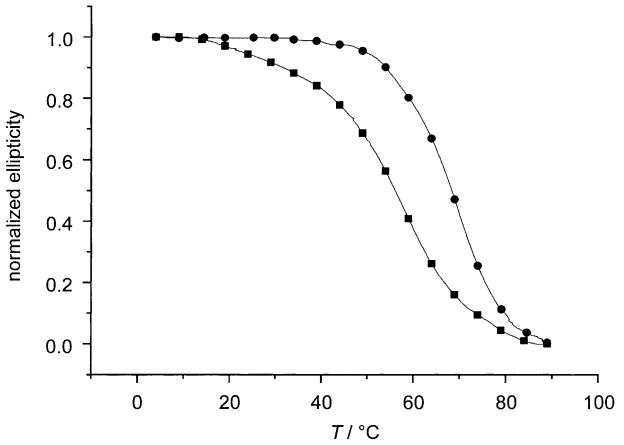

Figure 5. Thermal unfolding of trimer **II** (●) and trimer **IV** (■) monitored by CD at 225 nm with a heating rate of 0.2 °C min^{-1} at 4×10^{-5} M concentration in 20 mM phosphate buffer (pH 3.0).

remarkably less efficient than the C-terminal disulfide bridging of trimer **II.** This is proven by the 10 °C lower T_m value (Table 1). Even more surprising is the different shape of the thermal transition curves, which would suggest a significantly less cooperative unfolding of trimer **IV** compared to trimer **II**. A similarly reduced conformational stability has recently been reported for a (Gly-Pro-Pro)$_{10}$ construct with the N-terminal collagen III cystine knot expressed in *E. coli* when compared with the identical C-terminally cross-linked construct.[9]

Molecular modelling

We performed molecular dynamics simulations of trimers **II** and **IV** in a water box for two possible disulfide connectivities (Scheme 2). The other theoretically possible combinations were excluded on the basis that cystine bridges would have to be formed between cysteines that are quite spatially distant in a triple-helical conformation. In the synthesis of the trimers efficient oxidation is performed under conditions where the monomers are self-associated into a triple helix, and it therefore seems extremely unlikely that very distant cysteines would form a disulfide bond. MD simulations were also performed for a (Pro-Hyp-Gly)$_{11}$ trimer where the cystine knot was placed in the middle of the trimer to investigate the compatibility of a cystine knot in a triple-helical conformation. In previous modelling experiments based on visual inspection,[2b] it was concluded that the type A knot of Scheme 2 represents the natural cystine connectivities. The computer simulations suggest that neither cystine knot is compatible with a triple-helical conformation. However, in the simulations of trimer **II** with its C-terminal disulfide cross-links, both types of cystine connectivities allow a triple-helical conformation of the (Pro-Hyp-Gly) triplet directly adjacent to the knot. Since dihedral anlges of the cystine knot itself deviate only moderately from those of the triple-helical conformation, a possible induction of this structure by the C-terminal cystine knot is supported by the simulations. Contrarily, for the N-terminal cystine knot of trimer **IV** large deviations of the dihedral angles from those of a triple-helical conformation are observed. Even the first (Pro-Hyp-Gly) triplet is significantly distorted compared to an ideal triple helix. The experimentally observed lower stability and lower synthetic accessibility of trimer **IV** compared to trimer **II** is thus rationalised in terms of a lower compatibility of the cystine knot with the triple helix when placed at the N-terminus in the mode we chose for trimer **IV**. A definite statement regarding which cystine knot of Scheme 2 is the one present in the synthesised trimers cannot be made on the basis of the MD simulations. Type B of Scheme 2 seems more compatible with the triple-helical conformation in terms of dihedral angles, whilst type A represents the intuitively simplest way of forming the three disulfide bonds and leads to a conformation that, from visual inspection, seems closer to the triple helix.

NMR analysis

Measurement of experimental temperature dependences of NMR chemical shifts for trimer **II** resulted, for all glycines of the five (Pro-Hyp-Gly) repeats, in values more positive than -4.5 ppb K^{-1} (Figure 6) indicating involvement in hydrogen bonding as expected for a triple-helical structure. Conversely, the glycines C-terminal of the cystine knot seem to be unstructured as judged from their chemical shift and temperature shift coefficients. Surprisingly, no NMR signals were observed for the Cys residues below 70 °C, a fact that can only be explained by strong exchange broadening. The ^{1}H NMR spectra contain only few broad, but well-defined, resonances indicating the presence of only one homogeneous conforma-

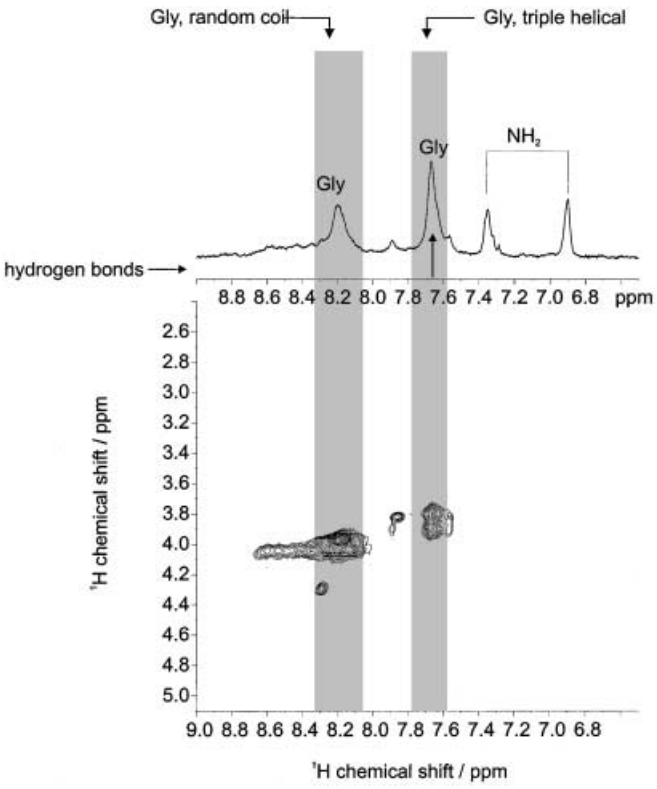

Figure 6. Fingerprint-region (amide/aliphatic) of the 2D-TOCSY NMR spectrum for trimer **II** recorded in water at 10 °C at 500 MHz. The corresponding section of the 1D ^{1}H spectrum is given on top. Vertical arrow below the 1D spectrum marks amide resonances that exhibit a temperature shift indicative of hydrogen bonding (> -4.5 ppb K^{-1}).

tional arrangement adopted by all molecules. The higher thermostability of trimer **II** as compared to trimer **VI** as well as a similar cooperativity in folding/unfolding for both trimers is also confirmed by ^{1}H NMR temperature series (data not shown). The cystine connectivities could not be identified and thus an unambiguous assignment to one of the two most plausible isomers according to modelling experiments (Scheme 2) was not possible.

Thermodegradation of the cystine knot

As already observed in the case of the collagenous trimer **VI** (Figure 1), which is C-terminally cross-linked by a simple artificial cystine knot,[6] even thermal unfolding of the trimers **II**–**IV** in water or phosphate buffer (pH 7.2) leads to thermodegradation of the more complex cystine knot. This is accompanied by almost quantitative scrambling of the disulfides. Because of the presence of two adjacent Cys residues, the decomposition products differ from those obtained in the case of trimer **VI**.[6] In fact, only monomeric species were identified by mass spectrometry which consist of the intrachain-disulfide bridged monomer, the related lanthionine molecule generated by loss of a sulphur atom and, most surprisingly, of a trisulfide species (Scheme 3). Although intramolecular disulfide-linked adja cent cysteine residues are rarely encountered in natural peptides and proteins,[18] this species was already observed in the thermolysis of trimer **VI** with the α2 chain containing two adjacent cysteine residues

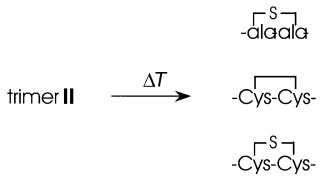

Scheme 3. Thermal decomposition of trimer **II** into three components as determined by LC-ESI-MS.

(Figure 1).[6] The loss of a sulphur atom on heating disulfide-bridged proteins with formation of lanthionine has been reported for wool.[19] The most probable mechanism consists of β elimination of cystines, as is known to occur for proteins under alkaline conditions,[20] but also under neutral conditions at high temperatures,[21] followed by re-addition of a cysteine thiol.[20b] However, more surprising was the formation of a trisulfide, a species which has been identified more recently in increasing numbers of natural products,[22] but has already been found in hydrolysates of wool.[23] Thermolysis of diacetyl-cystine bismethylamide as a model compound in neutral and alkaline conditions was found to generate both the cystine trisulfide and lanthionine species.[24]

As observed in the case of proteins[21] as well as in the preceding study on the collagen peptides with the artificial cystine knot,[6] thermodegradation was fully suppressed in the presence of Cu^{2+} ions. These facilitate spontaneous reoxidation of traces of thiols[12] generated on heating by means of the β elimination process,[21b] and in an even more efficient manner by lowering the pH to 3.0.

Folding kinetics of trimer II

By use of the temperature-jump technique, refolding kinetics of monomer **2a** (1 mM concentration) and of the two trimers **II** and **VI** (4×10^{-5} M concentration) in phosphate buffer (pH 3.0) were comparatively analysed at different temperatures. The activation energies (Table 2) were extracted from Arrhenius plots.

Table 2. Refolding rate constants of collagenous peptides after a temperature jump from 90 °C to different temperatures as monitored by CD at 225 nm in 20 mM phosphate buffer (pH 3) and the activation energies derived from the Arrhenius plots.

Collagen peptides	k [10^{-3} s^{-1}]					E_a
	4 °C	8 °C	12 °C	20 °C	40 °C	[kJ mol^{-1} K^{-1}]
trimer **II**[a]	1.06			3.76	9.39	43.5
trimer **VI**[a]	1.26			3.95	11.45	44.1
monomer **2a**[b]	0.429	0.645	0.79			50.2

[a] Concentration 4×10^{-5} M. [b] Concentration 1×10^{-3} M.

As shown in Figure 7, the refolding rate of trimer **VI** at 4 °C is slightly higher than that of trimer **II** with the natural cystine knot, but both refold significantly faster than monomer **2a**. Refolding of the two cross-linked trimers at 4 °C shows a fast, kinetically unresolved first phase with an amplitude of about 50 %, followed by a slower phase which is best fit by a first-

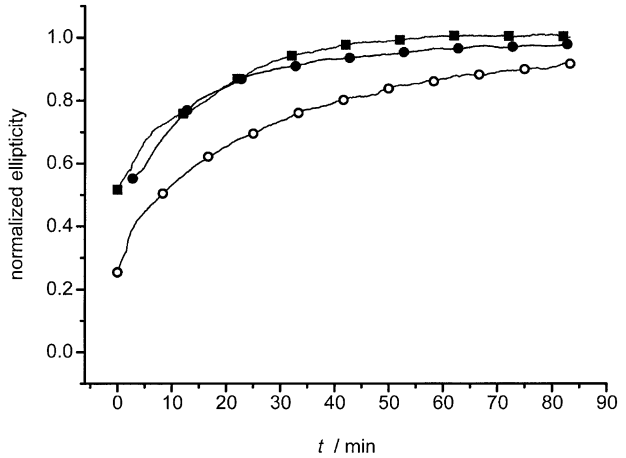

Figure 7. Refolding of monomer **2a** at 1×10^{-3} M (○), trimer **II** (●) and trimer **VI** (■) at 4×10^{-5} M concentration in 20 mM phosphate buffer (pH 3) as monitored by CD at 225 nm after a temperature jump from 90 to 4 °C.

order rate law. Refolding of the monomer **2a** shows a fast first phase of only 25% amplitude and the second slower phase again follows a first-order rate law. This would indicate that at the 1 mM concentration used the association of monomers to trimeric intermediates is not rate limiting. Nonetheless the rate constant of refolding of monomer **2a** is about 2.5 times slower than those derived for the two trimers (Table 2). Rather surprisingly, in the case of $(Pro\text{-}Pro\text{-}Gly)_{10}$ the rate constant ($0.7 \times 10^{-4}\,s^{-1}$) was found to be faster than that of the related construct with the C-terminal cystine knot ($0.12 \times 10^{-4}\,s^{-1}$) at 1 mM and 6×10^{-4} M concentration, respectively.[5] These conditions are very similar to those applied in the present study. However, the rate constant of trimer **II** at 20 °C ($3.95 \times 10^{-3}\,s^{-1}$) correlates well with that determined at this temperature for the fragment Col 1-3 of type III procollagen containing an identical cystine knot ($8 \times 10^{-3}\,s^{-1}$).[2b] Trimers **II** and **VI** exhibit higher rate constants than the model peptides containing the collagen type III knot and $(Pro\text{-}Pro\text{-}Gly)_{10}$ repeats[5, 10] or the artificial cystine knot and natural collagen sequences.[3b, 25] These sequence compositions are known to possess lower triple-helix propensities than the (Pro-Hyp-Gly) repeats of compounds **II** and **VI**. By comparing the activation energies, the almost identical values extracted from the Arrhenius plots for the trimers **II** and **VI** (Table 2) suggest a minimal effect of the type of cystine knot and thus confirm that *cis/trans* isomerisation steps of proline imide bonds are the rate limiting process.[5] The activation energies derived for trimers **II** and **VI**, which were lower than for self-association of the monomer **2a**, confirm the nucleating role of the cystine knots. Moreover, separation of the activation energy into the enthalpic and entropic terms by Eyring plots results in values that could imply enthalpically favoured, but entropically disfavoured isomerisation of the Pro/Hyp imide bonds in the formation of the triple helix (Table 3). Assignment of the activation enthalpies and entropies to the Pro/Hyp isomerisation steps is suggested by the ΔG values which are close to those reported for model Pro-peptides: 85 ± 10 kJ mol^{-1}.[26]

Table 3. Activation enthalpies ($\Delta H^{\neq}$) and entropies ($\Delta S^{\neq}$) as derived from Eyring plots. Additionally the free energy of activation at 300 K ($\Delta G^{\neq}_{300\,K}$) is given.

Collagen peptides	$\Delta H^{\neq}$ [kJ mol^{-1}]	$\Delta S^{\neq}$ [J mol^{-1} K^{-1}]	$\Delta G^{\neq}_{300\,K}$ [kJ mol^{-1}]
trimer **II**[a]	+41.1	−152.2	+86.8
trimer **VI**[a]	+41.7	−149.0	+86.4
monomer **2a**[b]	+47.8	−135.7	+88.5

[a] Concentration 4×10^{-5} M. [b] Concentration 1×10^{-3} M.

Thermodynamics of the folding/refolding processes of the trimers

By preventing thermolysis of the cystine knots under weakly acidic conditions, the potential contribution of these side reactions to the overall thermal unfolding process is excluded. Since the T_m values of trimer **II** are identical at pH 7.2 in the presence or absence of Cu^{2+} ions, scrambling of the disulfide knot to a higher extent occurs only at the high temperatures of the last unfolding step. As a consequence, this side reaction is not expected to affect the unfolding process itself; it just makes the process irreversible. Conversely, at pH 3 the process is fully reversible as shown in Figure 8 for trimer **II** where, after thermal unfolding, refolding occurs with only a minimum of kinetic hysteresis at the cooling rate

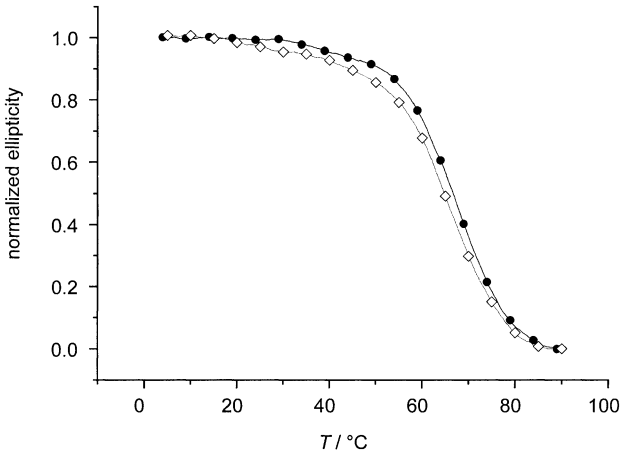

Figure 8. Thermal unfolding (●) and refolding (□) of trimer **II** at 4×10^{-5} M concentration in 20 mM phosphate buffer (pH 3.0) as monitored by CD at 225 nm.

applied. The related thermodynamic parameters are listed in Table 1. Thermodynamic data extracted at pH 7.2 in the absence of Cu^{2+} were found to be identical, within experimental error, to those derived in the presence of Cu^{2+} (data not shown) or at pH 3.0.

The structural stabilisation of trimer **II** by the natural cystine knot of collagen type III is compared in Figure 4 with the effects of the artificial cystine knot of trimer **VI** whose single chains share the identical $(Pro\text{-}Hyp\text{-}Gly)_5$ sequence. The triple helix of trimer **II** with its three disulfide cross-links exhibits a melting temperature that is 13 °C higher than that of trimer **VI** with two disulfide bridges. The cooperativity of the unfolding process of the triple helices of both trimers is practically identical, since the transition traces show parallel slopes. This was also confirmed by NMR experiments (see above).

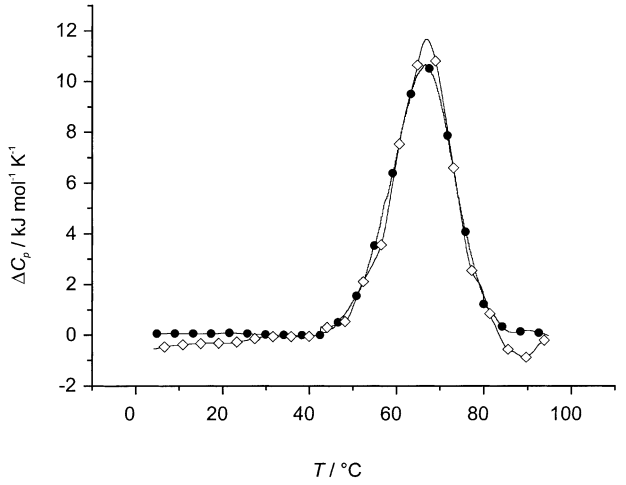

Figure 9. Thermal unfolding (●) and refolding (□) of trimer **II** at 4×10^{-5} M concentration in 20 mM phosphate buffer (pH 3.0) as monitored by DSC.

Microcalorimetric monitoring of the unfolding/refolding processes of the trimers at pH 3.0 yields symmetrical thermograms as shown in Figure 9 for trimer **II**, and the extracted thermodynamic parameters are listed in Table 4. It is conceivable that the different effects of the natural and artificial cystine knots on the triple-helix stability derive mainly from the entropy term. The more flexible artificial cystine knot of trimer **VI** with only two disulfide bridges could allow for a significant increase in entropy in this part of the molecule upon denaturation, while the three disulfide bridges of trimer **II** constrain the C-terminus in a fixed conformation. However, the expected differences in ΔH and ΔS are within experimental error.

Table 4. Thermodynamic parameters extracted from the thermal denaturation curves monitored by DSC for the collagen peptides at 4×10^{-5} M concentration in 20 mM phosphate buffer, pH 3.0.

Collagen peptides	Process	T_m [°C]	ΔH_{cal}[kJ mol^{-1}]	ΔS_{cal}[J mol^{-1} K^{-1}]
trimer **II**	unfolding	66.2	+202	+596
	refolding	66.5	−212	−625
	2nd unfolding	65.8	+203	+600
trimer **VI**[a]	unfolding	55.7	+191	+583
	refolding	54.5	−204	−623
	2nd unfolding	55.7	+202	+613

[a] Reported from the preceding article[6] for comparison.

Discussion

Protein folding and disulfide bond formation are thermodynamically coupled processes. They proceed through a prefolded precursor mechanism in which local regions of the protein adopt native structures that are then stabilised by the formation of disulfide bonds, while non-native disulfides are reshuffled with concurrent refolding.[27] Collagenous peptides built up of a sufficient number of (Xaa-Yaa-Gly) repeats with Xaa = Pro and Yaa = Pro/Hyp are known to self-associate into the collagen characteristic triple helix.[8a,b, 17, 28] This is then stabilised mainly by hydrogen-bonding of the Gly amide NHs to the Pro carbonyls in position Xaa of the adjacent chain in a very regular pattern. In solution, a concentration and temperature dependent equilibrium is established between self-associated fully matched triple-helical homotrimers with the maximum of possible hydrogen bonds exploited and monomeric unfolded chains according to the two-state model. However, mismatched trimers with a non-optimal hydrogen bonding pattern cannot be excluded. In the present study, the main intent was to investigate whether, even in collagens, formation of the native cystine knot is coupled to the folding process or whether it represents a post-folding event that serves to stabilise the triple helix.

N-terminally cross-linked (Gly-Pro-Hyp)$_3$ has been reported to form an incipient triple helix.[8a] However, air-oxidation of peptide **1b** failed to produce the interchain-disulfide knot to any detectable extent, even using a 1 mM peptide solution which is expected to minimise the concentration-dependency of homotrimerisation.[17] Conversely, with peptide **2b** which self-associates into homotrimers, as confirmed by the circular dichroic properties of the precursor **2a**, oxidation generates the disulfide cross-linked trimer **II** in relatively high yields. Since only a very low percentage of monomer **2b** is not structured as a triple helix (Figure 4) at the temperature selected for the oxidation experiments (7–8 °C), it was surprising to note that independently of the experimental conditions applied, a maximum of ≈70% correctly oxidised trimer **II** was obtained. This would strongly support a kinetically and not thermodynamically driven product distribution where intrachain disulfide bridging occurs at rates competing with the cystine knot formation. In this context, addition of the glutathione redox system at a peptide/GSH/GSSG ratio of 1:9:0.9 was expected to reduce non-productive intermediates and thus to reshuffle them into the trimeric species. However, *S*-glutathionylated species as reshuffling intermediates could not be detected by HPLC-MS in the course of the oxidation experiments, and the yields of trimer **II** could not be increased. This lack of reshuffling may derive from highly stable intrachain disulfides or from their steric inaccessibility. The latter explanation is strongly supported by the difficult accessibility of the cysteine residues in self-associated trimeric collagenous peptides for regioselective reactions,[6, 29] but also by the observation that only oxidised monomeric species are formed besides trimer **II**.

In agreement with studies on collagenous peptides,[8b, 11] the sequence composition of the N- and C-terminally capped peptide **2b** with five (Pro-Hyp-Gly) triplets represents the minimum size for a stable homotrimerisation, and thus at equilibrium the fraction of mismatched trimers that could also be a source of incorrectly oxidised products should be negligible. In the case of peptide **3b** with its seven triplets, formation of mismatched trimers at the temperature used in the oxidation experiments (7–8 °C) is conceivable and could well represent an additional limiting factor for correct interchain disulfide formation. However, again ≈70% was the upper limit of correctly oxidised trimer **III** and only intrachain oxidised monomers were detectable as side-prod-

ucts, thus further supporting the concept of kinetic control of the product distribution.

The results of the oxidation experiments would suggest that in the case of collagen peptides, folding and oxidation are not coupled processes, but that the triple-helical structure can only be stabilised by the disulfide-bond formation subsequent to proper folding. This is further supported by the almost identical conformational enthalpy determined for the self-associated peptide **2b** and the related cross-linked trimer **II**, while the entropy term dictates the significantly enhanced thermostability of the disulfide-bridged trimer (Table 1).

In contrast to observations for trimer **VI** where the triple helix propagates partially into the artificial knot,[6] in the case of trimer **II** such involvement of the cystine knot was not observed by NMR analysis and computer simulations. Comparing trimer **II** with its collagen type III cystine knot and trimer **VI** with only two disulfide bonds (Table 1), it can be concluded that the slightly enhanced conformational enthalpy deriving from the extension of the triple helix into the cystine knot in trimer **VI** is overcompensated for by the greater flexibility of the artificial knot. By the entropy gain obtained upon thermal unfolding, this leads to a lower thermostability. The higher flexibility of the artificial cystine knot and its better fit into the triple helix may explain the enhanced refolding rate of trimer **VI** compared to trimer **II** and thus the more efficient nucleation of the triple helix by the former one. This property is beneficial in terms of kinetics, whereas the activation energies for triple helix formation in both trimers seem to be fully dominated by the *cis/trans* isomerisation processes (Table 2 and Table 4).

Using Kemp′s triacid as a scaffold to cross-link N-terminally collagenous peptides, a flexible glycine residue was used as spacer to allow the correct registration of the chains.[8a,b] Despite this additional spacer, at least one (Gly-Pro-Hyp) triplet per chain was found to be only partially included into the triple helix.[8c] Similarly, incorporation of the cysteine residues at the Xaa and Yaa positions of the N-terminal triplet in peptide **4b**, producing three interchain disulfide bonds, is apparently not fully compatible with a triple-helix formation, since low yields of oxidised trimer **IV** were obtained. The resulting triple-helical structure was found to be of significantly lower thermostability. Most probably, insufficient spacing was introduced to avoid steric clashes for the onset of the triple helix. In fact, by incorporation of additional Gly and Ser residues as spacers in the polypeptide $GSYGPPGPCCGSGPP(GPP)_{10}$, expressed in *E. coli*, high yields of the correctly oxidised trimer were reported.[9] Also in this case a significantly reduced thermostability of the triple helix was observed. In collagen type XIII where the triple helix was proposed to propagate from the N- to the C-terminus,[7] oligomerisation is induced by a coiled-coil domain which, however, is spaced from the triple helix by a flexible hinge domain most probably to avoid steric clashes.

Conclusion

The results of this study fully support the conclusion of Engel and co-workers[5] that the collagen type III C-terminal cystine knot is readily obtained with properly designed collagenous peptides. It allows for the production of highly stable homotrimeric collagen mimics. Conversely, N-terminal cross-linking of collagen peptides by this cystine knot even in the proper design is not as efficient. Despite the facile synthetic accessibility of such homotrimeric collagenous peptides when compared to the use of synthetic templates, self-association of the peptide chains and proper folding is required for the correct oxidative cysteine pairings. Moreover, heterotrimeric collagen molecules still remain accessible only by a regioselective synthetic artificial cystine knot, which represents an efficient although laborious alternative.

Experimental Section

Peptide synthesis

Materials and methods: All reagents and solvents were of the highest quality commercially available and were used without further purification, except DMF, which was freshly distilled over ninhydrin. Amino acid derivatives were purchased from Fluka (Taufkirchen, Germany), TFFH from Aldrich (Taufkirchen, Germany) and the Rink-MBHA resin (linker: 4-[(*R,S*)-α-amino-2′,4′-dimethoxybenzyl]phenoxyacetylnorleucine-amido-benzhydryl) from Calbiochem-NovaBiochem (Läufelfingen, Switzerland). Peptide synthesis was performed manually in a polypropylene syringe fitted with a polyethylene disk. Precoated silica gel 60 TLC plates were from Merck AG (Darmstadt, Germany) and compounds were visualised with chlorine/tolidine or permanganate. Analytical RP-HPLC was performed with Waters equipment (Eschborn, Germany) using reversed-phase Nucleosil C18 columns (0.4 × 25 cm, 10 μm, Macherey & Nagel, Düren, Germany) and linear gradients of acetonitrile/2 % H_3PO_4 (from 5:95 to 90:10 in 15 min at a flow rate of 1.5 mL min^{-1}) as eluents. UV absorbance was monitored at 210 nm. Preparative RP-HPLC was carried out with Abimed equipment (Langenfeld, Germany) on reversed-phase Nucleosil C18 (2.1 × 25 cm, 5 μm endcapped) columns by elution with a linear gradient of acetonitrile (containing 0.08 % TFA)/0.1 % TFA from 2:8 to 8:2 in 50 min. Elution profiles were monitored by UV at 210 nm. For preparative size-exclusion column chromatography a 145/1.25 Fraktogel HSK HW-40 S column (145 × 1.25 cm) and isocratic elution with 0.5 % AcOH at a flow rate of 0.4 mL min^{-1} was used. ESI-MS were recorded on a PE Sciex API 165 from Perkin-Elmer and FT-ICR-MS on a 4.7 T APEX II (Bruker). Fmoc-Pro-Hyp(*t*Bu)-Gly-OH was synthesised as described previously.[3d]

General procedures: The Fmoc-protected Rink-MBHA resin (loading: 0.72 mmol g^{-1}) was treated with 20 % piperidine in DMF (1 × 15 min, 1 × 5 min) and then washed successively with DMF (3 × 1 min), MeOH (3 × 1 min), CH_2Cl_2 (3 × 1 min) and MeOH (3 × 1 min). Coupling of the first amino acid (Fmoc-Gly-OH) was performed with Fmoc-Gly-OH/HBTU/HOBt/DIEA (0.9 equiv, 1:1:1:2) in DMF (2 h) followed by washing with DMF (3 × 1 min), MeOH (3 × 1 min), CH_2Cl_2 (3 × 1 min), MeOH (3 × 1 min) and DMF (3 × 1 min). The resin was capped by acetylation with Ac_2O/DIEA (4 equiv, 1:1) and DMAP (0.1 equiv) in DMF (2 × 30 min). Loading of the resin with the first amino acid was determined spectroscopically by quantitation of the fulvene/piperidine adduct at 301 nm ($\varepsilon = 7800$) upon Fmoc removal under above conditions.

Chain elongation with Fmoc-amino acid was performed by double couplings with four equivalents Fmoc-Xaa-OH/HBTU/HOBt/DIEA (1:1:1:2) in DMF (2 × 1 h) followed by washings with DMF (3 × 1 min), MeOH (3 × 1 min), CH_2Cl_2 (3 × 1 min) and MeOH (3 × 1 min). Chain elongation with Fmoc-Pro-Hyp(*t*Bu)-Gly-OH was carried out by single couplings (2 h) with 1.8 equivalents of Fmoc-Pro-Hyp(*t*Bu)-Gly-OH/TFFH/DIEA (1:1:2) in DMF (in the first three coupling steps) and NMP/CH_2Cl_2 (in further coupling steps) followed by washings with DMF (3 × 1 min), acylation with $(Boc)_2O$ (10 equiv) in DMF (20 min) and additional washings with DMF (3 × 1 min), MeOH (3 × 1 min), CH_2Cl_2 (3 × 1 min) and MeOH (3 × 1 min). Coupling efficiency was monitored with the Kaiser test,[31] except for N-terminal proline residues where the chloranil test[32] was applied.

Fmoc-cleavage from Fmoc-Pro-peptidyl resin was carried out with 2% piperidine and 2% DBU in DMF (0 °C, 1 × 60 sec, 1 × 30 s) and washings with DMF (3 × 1 min), MeOH (3 × 1 min), CH_2Cl_2 (3 × 1 min) and MeOH (3 × 1 min). N-terminal acetylation of the peptides on resin was performed with four equivalents of Ac_2O/DIEA (1:2) in DMF (2 × 30 min) followed by washings with DMF (3 × 1 min), MeOH (3 × 1 min), CH_2Cl_2 (3 × 1 min) and MeOH (3 × 1 min).

Synthesis of the monomeric peptide-amides

Peptide synthesis was performed as described under general procedures using Fmoc-Gly-Rink-MBHA Resin (1 g, 0.4 mmol g^{-1}). Upon the 3rd, 5th and 7th coupling of Fmoc-Pro-Hyp(*t*Bu)-Gly-OH the resin was washed with DMF (3 × 1 min), MeOH (3 × 1 min), CH_2Cl_2 (3 × 1 min) and Et_2O (3 × 1 min) and dried. Aliquots of the resin were taken for N-terminal peptide acetylation with Ac_2O as reported under general procedures.

Ac-[Pro-Hyp-Gly]$_3$-Pro-Cys(S*t*Bu)-Cys(S*t*Bu)-Gly-Gly-Gly-NH$_2$ (1a): For deprotection/cleavage Ac-[Pro-Hyp(*t*Bu)-Gly]$_3$-Pro-Cys(S*t*Bu)-Cys-(S*t*Bu)-Gly-Gly-Gly resin (462 mg) was treated with TFA/Et_3SiH/H_2O (96:2:2; 1 × 15 min, 2 × 40 min, 1 × 60 min), filtered off and washed additionally with CH_2Cl_2. The combined filtrates were concentrated and the crude product was precipitated with Et_2O, collected by filtration and lyophilised from *t*BuOH/H_2O (5:1). Yield: 170 mg (83%); HPLC: t_R = 11.4 min (>85%); ESI-MS: *m*/*z*:756.4 $[M+2H]^{2+}$, 1511.6 $[M+H]^+$; M_r = 1511.84 calcd for $C_{63}H_{98}N_{16}O_{19}S_4$. For spectroscopic measurements a portion of the material was further purified by preparative HPLC as described under Materials and Methods (HPLC: >98%).

Ac-[Pro-Hyp-Gly]$_5$-Pro-Cys(S*t*Bu)-Cys(S*t*Bu)-Gly-Gly-Gly-NH$_2$ (2a): Deprotection/cleavage of Ac-[Pro-Hyp(*t*Bu)-Gly]$_5$-Pro-Cys(S*t*Bu)-Cys-(S*t*Bu)-Gly-Gly-Gly resin (520 mg) was carried out as described for compound **1a**. The product was precipitated with Et_2O and lyophilised from *t*BuOH/H_2O (5:1). Yield: 215 mg (79%); HPLC: t_R = 9.5 min (>85%); ESI-MS: *m*/*z*: 1023.4 $[M+2H]^{2+}$; M_r = 2046.41 calcd for $C_{87}H_{132}N_{22}O_{27}S_4$. For spectroscopic measurements a portion of the material was further purified by preparative HPLC as described under Materials and Methods (HPLC: >98%).

Ac-[Pro-Hyp-Gly]$_7$-Pro-Cys(S*t*Bu)-Cys(S*t*Bu)-Gly-Gly-Gly-NH$_2$ (3a): Deprotection and cleavage of the peptide from the resin (310 mg) was carried out as described for compound **1a**. The crude peptide was precipitated from the cleavage mixture with Et_2O, dissolved in *t*BuOH/H_2O (5:1) and lyophilised. The white solid was dissolved in MeOH and purified by preparative RP-HPLC. Fractions containing homogeneous product were combined, concentrated and lyophilised. Yield: 50 mg (14.5%); HPLC: t_R = 9.4 min (>95%); ESI-MS: *m*/*z*: 1291.6 $[M+2H]^{2+}$; M_r = 2580.98 calcd for $C_{111}H_{166}N_{28}O_{35}S_4$.

Ac-Cys(S*t*Bu)-Cys(S*t*Bu)-Gly-[Pro-Hyp-Gly]$_5$-Gly-Gly-Gly-NH$_2$ (4a): Peptide synthesis was performed on Fmoc-Gly-MBHA resin (275 mg; 0.4 mmol g^{-1}) as described under general procedures. The peptide was deprotected and cleaved from the resin and isolated as reported for compound **1a**. The crude product was dissolved in MeOH and purified by preparative RP-HPLC. Fractions containing homogeneous product were combined, concentrated and lyophilised from *t*BuOH/H_2O (5:1). Yield: 133 mg (60%); HPLC: t_R = 10.2 min (61.3%); ESI-MS: *m*/*z*: 1003.6 $[M+2H]^{2+}$; M_r = 2006.34 calcd for $C_{84}H_{128}N_{22}O_{27}S_4$. For spectroscopic measurements a portion of the material was further purified by preparative HPLC (>95%).

Ac-Cys(S*t*Bu)-Cys(S*t*Bu)-Gly-[Pro-Hyp-Gly]$_5$-Pro-Cys(S*t*Bu)-Cys(S*t*Bu)-Gly-Gly-Gly-NH$_2$ (5a): The title compound was synthesised on Fmoc-Gly-MBHA resin (275 mg; 0.4 mmol g^{-1}) as reported under General Procedures, cleaved/deprotected and isolated as compound **1a**. Yield: 153 mg (56%); HPLC: t_R = 11.6 min (36%); ESI-MS: *m*/*z*: 1243.6 $[M+2H]^{2+}$; M_r = 2486.09 calcd for $C_{103}H_{161}N_{25}O_{30}S_8$. Homogeneous material (HPLC >95%) was obtained by preparative HPLC.

Synthesis of the homotrimer II

Ac-(Pro-Hyp-Gly)$_5$-Pro-C^{l}ys-C^{l}ys-Gly-Gly-Gly-NH$_2$ (2b): Tributylphosphine (0.98 mmol, 0.24 mL) was added to peptide **2a** (100 mg, 49 μmol) in TFE/H_2O (95:5, 100 mL) and the solution was stirred at RT for 5 h. The mixture was concentrated and the peptide precipitated with cold Et_2O. The residue was lyophilised from *t*BuOH/H_2O (4:1); yield: 81.5 mg (89%); HPLC: t_R = 7.3 min (>95%); ESI-MS: *m*/*z*: 936.6 $[M+2H]^{2+}$; M_r = 1870.06 calcd for $C_{79}H_{116}N_{22}O_{27}S_2$.

[Ac-(Pro-Hyp-Gly)$_5$-Pro-C^{l}ys-C^{l}ys-Gly-Gly-Gly-NH$_2$]$_3$ (II): An argon-saturated solution of peptide **2b** (15 mg, 8.02 μmol) in 25 mM NH_4Ac, pH 8.0 (15 mL) was kept at 4 °C for 5–7 h. It was then gently stirred under air oxygen at RT for 5–7 days with continuous monitoring of the oxidative process by ESI-MS and Grassetti test.[33] After completion of the reaction, the solution was lyophilised and the product purified by size-exclusion chromatography. Yield: 3.4 mg (22.7%); HPLC: t_R = 7.2 min (>95%); ESI-MS: *m*/*z*: 1869.4 $[M+3H]^{3+}$, 1402.2 $[M+4H]^{4+}$, 1122.0 $[M+5H]^{5+}$; M_r = 5604.18 calcd for $C_{237}H_{342}N_{66}O_{81}S_6$.

Synthesis of the homotrimer III

Ac-[Pro-Hyp-Gly]$_7$-Pro-Cys-Cys-Gly-Gly-Gly-NH$_2$ (3b): Compound **3a** (30 mg, 11.6 μmol) was allowed to react in TFE/H_2O (95:5, 30 mL) with tributylphosphine (233 μmol, 57 μL) at RT for 5 h and the product was isolated as reported for **2b**. Yield: 24.3 mg (87%); HPLC: t_R = 7.2 min (>87%); ESI-MS: *m*/*z*: 1203.2 $[M+2H]^{2+}$, 802.4 $[M+3H]^{3+}$; M_r = 2404.64 calcd for $C_{103}H_{150}N_{28}O_{35}S_2$.

[Ac-(Pro-Hyp-Gly)$_7$-Pro-C^{l}ys-C^{l}ys-Gly-Gly-Gly-NH$_2$]$_3$ (III): An argon-saturated solution of **3b** (24 mg, 10 μmol) in 25 mM NH_4Ac, pH 8 (24 mL) was kept at 4 °C for 7 h and then gently stirred under air oxygen for 5–7 days. The reaction mixture was worked up and the crude product purified by size-exclusion chromatography as described for trimer **II**. Yield: 8.7 mg (36%); HPLC: t_R = 6.95 min (>95%); ESI-MS: *m*/*z*: 1803.2 $[M+4H]^{4+}$, 1442.6 $[M+5H]^{5+}$; M_r = 7207.92 calcd for $C_{309}H_{444}N_{84}O_{105}S_6$.

Synthesis of the homotrimer IV

Ac-Cys-Cys-Gly-(Pro-Hyp-Gly)$_5$-Gly-Gly-Gly-NH$_2$ (4b): Compound **4a** (25 mg, 12.5 μmol) was allowed to react in TFE/H_2O (95:5, 25 mL) with tributylphosphine (250 μmol, 61 μL) at RT for 5 h and the product was isolated as reported for **2b**. Yield: 21 mg (91%); HPLC: t_R = 6.35 min (>85%); ESI-MS: *m*/*z*: 916.2 $[M+2H]^{2+}$; M_r = 1830.00 calcd for $C_{76}H_{112}N_{22}O_{27}S_2$.

[Ac-C^{l}ys-C^{l}ys-Gly-(Pro-Hyp-Gly)$_5$-Gly-Gly-Gly-NH$_2$]$_3$ (IV): The title compound was prepared by air oxidation of the peptide **4b** (21 mg, 11.4 μmol) in 25 mM NH_4Ac buffer, pH 8.0 (21 mL) upon overnight equilibration of the solution under argon at 4 °C. The product was isolated by size-exclusion chromatography. Yield: 273 μg (1.3%); HPLC: t_R = 6.26 min (>98%); ESI-MS: *m*/*z*: 1372.2 $[M+2H]^{4+}$; M_r = 5484.00 calcd for $C_{228}H_{330}N_{66}O_{81}S_6$.

CD measurements: The CD spectra were recorded on a Jasco J-715 spectropolarimeter equipped with a thermostated cell holder and connected to a PC for signal averaging and processing. All spectra were recorded in the 190–250 nm range employing quartz cuvettes of 0.1 cm optical path length. The average of 10 scans is reported and expressed in terms of ellipticity units per mole of peptide residues ($[\Theta]_R$). The measurements were performed on peptide solutions pre-equilibrated at 4 °C for at least 12 h, at a concentration of 4×10^{-5} M for the trimers and 1 mM for the self-associated single chains in water, 20 mM phosphate (pH 7.2) in the absence and presence of 1×10^{-5} mM $CuCl_2$ (the precipitated copper hydroxide was filtered off) and in 20 mM phosphate buffer at pH 3.0. The concentrations were determined by weight and a peptide content of about 80% in analogy to previously synthesised collagenous peptides of similar sequence composition. The thermal denaturation curves were monitored following the change in intensity of the circular dichroic signal at 225 nm in thermal excursion from 4 to 90 °C with a heating rate of 0.2 °C min^{-1}. T_m values and thermodynamic parameters were derived from original transition curves using the JASCO software.

For refolding kinetics 10 mM solutions of compound **2a** and 4×10^{-4} M solutions of trimers **II** and **III** in 20 mM phosphate buffer (pH 3.0) were kept at 90 °C for 15 min to achieve total denaturation. Aliquots (10 μL) were taken and diluted in thermostated buffer to 1 mM solutions of **2a** and 4×10^{-5} M solutions of trimers **II** and **III**. After a dead time of 10 s registration of the circular dichroic intensity at 225 nm served to monitor refolding at the chosen temperatures. For the Arrhenius plots refolding was performed at 4, 20 and 40 °C for trimers **II** and **III**, and at 4, 8 and 12 °C for peptide **2b**.

DSC measurements: The temperature dependence of the partial heat capacity was determined on a VP-DSC microcalorimeter (MicroCal, Northampton, USA) equipped with a cell feedback network and two fixed-in-place cells with effective volumes of approximately 0.5 mL. The measurements were carried out on 1 mM peptide solutions in the case of **2a** and at 4×10^{-5} M concentration for trimer **II** in 20 mM phosphate buffer at pH 3.0 with and without $CuCl_2$ (1 mM), after pre-equilibration at 4 °C for

at least 12 h. Thermal denaturations were recorded by monitoring the variation of the heat capacity (C_p) as a function of the increasing temperature (4–90 °C) using a scan rate of 0.2 °C min^{-1}. Data analysis was performed with the Origin software modified for microcalorimetric applications (MicroCal, Northampton, USA) using the two-state transition model.[34]

Crystallisation of the trimers: Crystallisation of trimers **II** and **III** was carried out at 4 °C using the hanging-drop vapour diffusion method. As precipitating agents PEG 200 and PEG 400 were used at concentrations ranging from 15 to 25 %. Initial concentration of trimers **II** and **III** was 5 mg per mL of 10 % aqueous AcOH.

NMR measurements: NMR experiments were carried out on a 2 mM sample of trimer **II** between 10 °C and 75 °C on Bruker DRX 500 and AMX 400 spectrometers. 2D-TOCSY[35] and 2D-NOESY[36] experiments were recorded in a H_2O/D_2O (9:1) mixture using the WATERGATE water suppression scheme.[37] Temperature shift coefficients for the amide protons were obtained from 1D spectra recorded between 10 and 30 °C to assure a triple-helical conformation.

Molecular modelling: Molecular modelling was performed on Silicon Graphics O2 R5000 computers (Silicon Graphics Inc., Mountain View, CA) with the INSIGHTII program package (Accelrys, San Diego, CA) using the CVFF force field. Molecular dynamics simulations of trimers **II** and **IV** were carried out in a water box of size $9 \times 3 \times 3$ nm^3 containing approximately 2400 water molecules. Starting from six (Pro-Hyp-Gly) repeats in ideal triple-helical conformation Hyp and Gly of the sixth triplet were replaced by cysteines followed by three glycines. N-and C-termini were capped by the acetyl and amide group, respectively. Disulfide bonds were created according to Scheme 2 and the two resulting molecules were minimised in the water box. From these starting conformations, molecular dynamics were simulated at 10 K for 10 ps followed by gradual heating (with time constant 1 ps) to 300 K over 100 ps. For comparison, the same simulations were performed with the identical cystine knot placed at the N-terminus. Additionally, for better evaluation of the compatibility of the cystine knot with the triple-helical conformation both cystine knots of Scheme 2 were placed in the middle of a $(Pro\text{-}Hyp\text{-}Gly)_{11}$ triple helix (again with Cys-Cys replacing the Hyp-Gly positions). In this case a water box of size $12 \times 3 \times 3$ nm^3 containing approximately 3100 water molecules was used and the same calculations were performed as described above. In all simulations step size was 1 fs and snapshots were saved each picosecond. Mainly backbone dihedral angles and rmsd of backbone atom coordinates were used for analysis of the trajectories.

Acknowledgement

This study was partly supported by the SFB 533 (grant A8) of the Ludwig-Maximilians-University of Munich and SFB 563 (grant C4) of the Technical University of Munich. We thank Dr. J. Engel, Biozentrum, Basel, for intensive and helpful discussions during this project and Dr. D. Schmid, Institute of Organic Chemistry, Tübingen, for recording the FT-ICR-MS spectra.

[1] a) E. Chung, E. M. Keele, E. J. Miller, *Biochemistry* **1974**, *13*, 3459–3464; b) R. W. Glanville, H. Allmann, P. P. Fietzek, *Hoppe-Seyler's Z. Physiol. Chem*. **1976**, *357*, 1663–1665.

[2] a) H. P. Bächinger, P. Bruckner, R. Timpl, D. J. Prockop, J. Engel, *Eur. J. Biochem.* **1980**, *106*, 619–632; b) P. Bruckner, H. P. Bächinger, R. Timpl, J. Engel, *Eur. J. Biochem.* **1978**, *90*, 595–603; c) H. P. Bächinger, P. Bruckner, R. Timpl, J. Engel, *Eur. J. Biochem*. **1978**, *90*, 605–613; d) J. Engel, H. P. Bächinger, P. Bruckner, R. Timpl in *Protein Folding* (Ed.: R. Jaenicke), Elsevier/North Holland, Amsterdam, **1980**, pp. 345–367; e) J. Engel, *Adv. Meat Res.* **1987**, *4*, 145–161.

[3] a) J. Ottl, R. Battistuta, M. Pieper, H. Tschesche, W. Bode, K. Kühn, L. Moroder, *FEBS Lett.* **1996**, *398*, 31–36; b) J. Ottl, L. Moroder, *J. Am. Chem. Soc*. **1999**, *121*, 653–661; c) J. C. D. Müller, J. Ottl, L. Moroder, *Biochemistry* **2000**, *39*, 5111–5116; d) B. Saccà, L. Moroder, *J. Peptide Sci.* **2002**, *8*, 192–204.

[4] D. E. Mechling, H. P. Bächinger, *J. Biol. Chem*. **2000**, *275*, 14532–14536.

[5] S. Boudko, S. Frank, R. A. Kammerer, J. Stetefeld, T. Schulthess, R. Landwehr, A. Lustig, H. P. Bächinger, J. Engel, *J. Mol. Biol.* **2002**, *317*, 459–470.

[6] D. Barth, H.-J. Musiol, M. Schütt, S. Fiori, A. G. Milbradt, C. Renner, L. Moroder, *Chem. Eur. J.* **2003**, *9*, 3692–3702, preceding paper.

[7] a) A. Snellman, H. Tu, T. Vaisanen, A. P. Kvist, P. Huhtala, T. Pihlajaniemi, *EMBO J.* **2000**, *19*, 5051–5059; b) S. K. Areida, D. P. Reinhardt, P. K. Müller, P. P. Fietzek, J. Kowitz, M. P. Marinkovich, H. Notbohm, *J. Biol. Chem.* **2001**, *276*, 1594–1601.

[8] a) M. Goodman, Y. Feng, G. Melacini, J. P. Taulane, *J. Am. Chem. Soc.* **1996**, *118*, 5156–5157; b) Y. Feng, G. Melacini, J. P. Taulane, M. Goodman, *J. Am. Chem. Soc.* **1996**, *118*, 10351–10358; c) G. Melacini, Y. Feng, M. Goodmann, *J. Am. Chem. Soc*. **1996**, *118*, 10359–10364; d) M. Goodman, M. Bhumralkar, E. A. Jefferson, J. Kwak, E. Locardi, *Biopolymers* **1998**, *47*, 127–142; e) E. T. Rump, D. T. S. Rijkers, H. W. Hilbers, P. G. de Groot, R. M. J. Liskamp, *Chem. Eur. J.* **2002**, *8*, 4613–4621; f) Y. Greiche, E. Heidemann, *Biopolymers* **1979**, *18*, 2359–2361.

[9] S. Frank, S. Boudko, K. Mizuno, T. Schulthess, J. Engel, H. P. Bächinger, *J. Chem. Biol.* **2003**, 278, 7747–7750.

[10] a) A. Rich, F. C. H. Crick, *J. Mol. Biol*. **1961**, *3*, 483–506; b) G. N. Ramachandran, *Treatise on Collagen*, Academic Press, New York, **1964**, pp. 103–183.

[11] P. Bruckner, B. Rutschmann, J. Engel, *Helv. Chim. Acta* **1975**, *58*, 1276–1287.

[12] Y. M. Torchinsky, *Sulfur in Proteins*, Pergamon Press, Oxford, **1981**.

[13] a) R. Berisio, L. Vitagliano, G. Sorrentino, L. Carotenuto, C. Piccolo, L. Mazzarella, A. Zagari, *Acta Crystallogr.* **2000**, *D56*, 55–61; b) R. Berisio, L. Vitagliano, L. Mazzarella, A. Zagari, *Biopolymers* **2001**, *56*, 8–13.

[14] a) K. Okuyama, K. Okuyama, S. Arnott, M. Takayanagi, M. Kakudo, *J. Mol. Biol.* **1981**, *152*, 427–443; b) J. Bella, M. Earon, B. Brodsky, H. M. Berman, *Science* **1994**, *266*, 75–81; c) R. Z. Kramer, L. Vitagliano, J. Bella, R. Berisio, L. Mazzarella, B. Brodsky, A. Zagari, H. M. Berman, *J. Mol. Biol.* **1998**, *280*, 623–638; d) V. Nagarajan, S. Kamitori, K. Okuyama, *J. Biochem.* **1998**, *124*, 1117–1123; e) V. Nagarajan, S. Kamitori, K. Okuyama, *J. Biochem.* **1999**, *125*, 310–318.

[15] a) K. H. Gustavson, *Acta Chem. Scand*. **1954**, *8*, 1298–1305; b) K. H. Gustavson, *Nature* **1955**, *175*, 70–74; c) S. Leikin, D. C. Rau, V. A. Parsegian, *Nature Struct. Biol.* **1995**, *2*, 205–210.

[16] a) E. Heidemann, W. Roth, *Adv. Polym. Sci*. **1982**, *43*, 143–203; b) C. G. Fields, C. M. Lovdahl, A. J. Miles, Y. C. Yu, V. L. M. Hagen, G. B. Fields, *Biopolymers* **1993**, *33*, 1695–1707; c) B. Grab, A. J. Miles, L. T. Furcht, G. B. Fields, *J. Biol. Chem.* **1996**, *271*, 12234–12240; d) T. Tanaka, Y.Wada, H. Nakamura, T. Doi, T. Imanishi, T. Kodama, *FEBS Lett.* **1993**, 334, 272–276; e) H. Hoyo, Y. Akamatsu, K. Yamauchi, M. Kinoshita, *Tetrahedron* **1997**, *53*, 14263–14274; f) W. Henkel, T. Vogl, H. Echner, W. Voelter, G. Urnbanke, D. Schleuder, J. Rautenberg, *Biochemistry* **1999**, *38*, 13610–13622; g) T. Koide, M. Yuguchi, M. Kawakita, H. Konno, *J. Am. Chem. Soc.* **2002**, *124*, 9388–9389.

[17] J. Engel, H.-T. Chen, D. J. Prockop, H. Klump, *Biopolymers* **1977**, *16*, 601–602.

[18] a) C. J. Creighton, C. H. Reynolds, D. H. S. Lee, G. C. Leo, A. B. Reitz, *J. Am. Chem. Soc.* **2001**, *123*, 12664–12669; b) T. Kimura, *Methods of Organic Chemistry*, Houben-Weyl, **2002**, E22b, pp. 142–161.

[19] R. D. Süssmuth, R. W. Jack, G. Jung, *Methods of Organic Chemistry*, Houben-Weyl, **2002**, E22b, pp. 186–213.

[20] a) T. M. Florence, *Biochem. J.* **1980**, *189*, 507–520; b) J. R. Whitaker, R. E. Feeney, *CRC Crit. Rev. Food Sci. Nutr.* **1983**, *19*, 173–212.

[21] a) T. J. Ahern, A. M. Klibanov, *Science* **1985**, *228*, 1280–1284; b) S. A. Zale, A. M. Klibanov, *Biochemistry* **1986**, *25*, 5432–5444; c) D. B. Volkin, A. M. Klibanov, *J. Biol. Chem.* **1987**, 262, 2945–2950.

[22] H.-J. Musiol, G. Loidl, L. Moroder, *Methods of Organic Chemistry*, Houben-Weyl, **2002**, E22b, pp. 179–183.

[23] J. C. Fletcher, A. Robson, *Biochem. J.* **1963**, *87*, 553–559.

[24] M. Ghadimi, R. R. Hill, *J. Chem. Soc. Chem. Commun.* **1991**, 903.

[25] B. Saccà, C. Renner, L. Moroder, *J. Mol. Biol.* **2002**, *324*, 309–318.

[26] F. X. Schmid, *Annu. Rev. Biophys. Biomol. Struct.* **1993**, 22, 123–143

[27] a) T. E. Creighton, *Meth. Enzymol.* **1986**, *131*, 83–106; b) T. E. Creighton, *Protein Folding* (Ed.: T. E. Creighton), W. H. Freeman, New York, **1992**, pp. 301–351,

[28] a) S. Sakakibara, K. Inouye, K. Shuda, Y. Kishida, Y. Kobayashi, D. J. Prockop, *Biochim. Biophys. Acta* **1973**, *303*, 198 – 202; b) K. Inouhe, S. Sakakibara, D. J. Prockop, *Biochim. Biophys. Acta* **1976**, *420*, 133 – 141; c) K. Inouhe, Y. Kobayashi, Y. Kyogoku, Y. Kishida, S. Sakakibara, D. J. Prockop, *Arch. Biochem. Biophys.* **1982**, *219*, 198 – 203.
[29] B. Saccà, D. Barth, H.-J. Musiol, L. Moroder, *J. Pept. Sci*. **2002**, *8*, 205 – 210.
[30] J. Engel, D. J. Prockop, *Annu. Rev. Biophys. Biophys. Chem*. **1991**, *20*, 137 – 152.
[31] E. Kaiser, R. L. Colescott, C. D. Bossinger, P. I. Cook, *Anal. Biochem.* **1970**, *34,* 595 – 598.
[32] T. Christensen in *Peptides, Structure and Biological Functions.* Proceedings of the 6th American Peptide Symposium (Eds.: E. Gross, J. Meienhofer), Pierce Chemical Co.: Rockford, Il., **1979**, pp. 385 – 388.
[33] D. R. Grassetti, J. F. Murray, *Arch. Biochem. Biophys.* **1967**, *119*, 41 – 49.
[34] P. L. Privalov, *Adv. Protein Chem.* **1982**, *35*, 1 – 104.
[35] A. Bax, D. G. Davis, *J. Magn. Reson*. **1985**, *65*, 355 – 360.
[36] J. Jeener, B. H. Meier, P. Bachman, R. R. Ernst, *J. Chem. Phys.* **1979**, *71*, 4546 – 4553.
[37] V. Sklenar, M. Piotto, R. Leppik, V. J. Saudek, *J. Magn. Reson. Ser. A* **1993**, *102,* 241 – 245.

Received: March 4, 2003 [F4918]